Computed tomography (CT)

Part 1

J. Kybic, A. Sopczak[1]

Department of cybernetics, FEE CTU
http://cmp.felk.cvut.cz/~kybic
kybic@fel.cvut.cz

2005–2024

[1] Using images from J. Hozman, J. Fessler, S. Webb, M. Slaney, A. Kak and others

Introduction to CT

Hardware

Mathematics and Physics of CT

Radon transform

Computed Tomography (CT) scanner

CT history

1917 mathematical theory (Radon)
1956 tomography reconstruction in radioastronomy (Bracewell)
1963 CT reconstruction theory (Cormack)
1971 CT principles demonstrated (Hounsfield)
1972 first working CT for humans (EMI, London, Hounsfield)
1973 PET, Positron Emission Tomography
1974 Ultrasound tomography
1975 whole body scanner (Hounsfield)
1982 Single Photon Emission Computed Tomography (SPECT)
1985 Helical CT
1998 Multislice CT, 0.5 s/frame

Johann Radon

1887–1956

- born in Děčín (Czech Republic), lived in Göttingen, Brno, Hamburg, Greifswald, Erlangen, Breslau, Innsbruck and Vienna
- mathematician; Radon transform (1917) — reconstruction of a function from its integrals on certain manifolds (projections)

Godfrey Hounsfield

1919–2004

- physicist and engineer (did not attend university)
- worked on radar and on first transistor computers
- created the first CT X-ray scanner
- Nobel prize in Medicine (1979, together with Cormack)

Allan MacLeod Cormack

1924–1998

- born in South Africa, studied in Cambridge, lived in the US
- particle physicist
- theoretical foundation of CT scanning (independently of Hounsfield)
- Nobel prize in Medicine (1979, together with Hounsfield)

CT principles

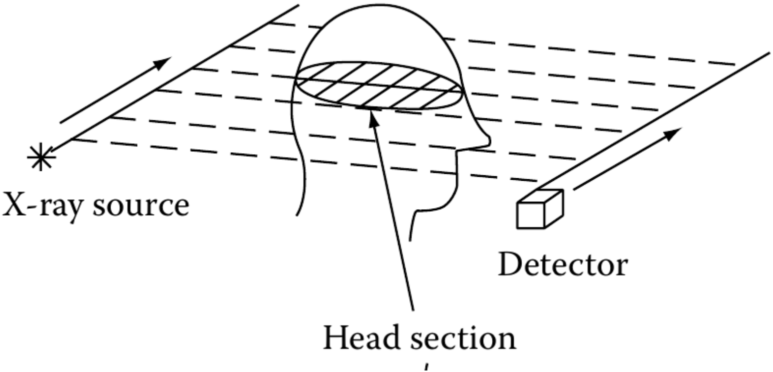

1. Sequence of parallel sections *(tomos)*

CT principles

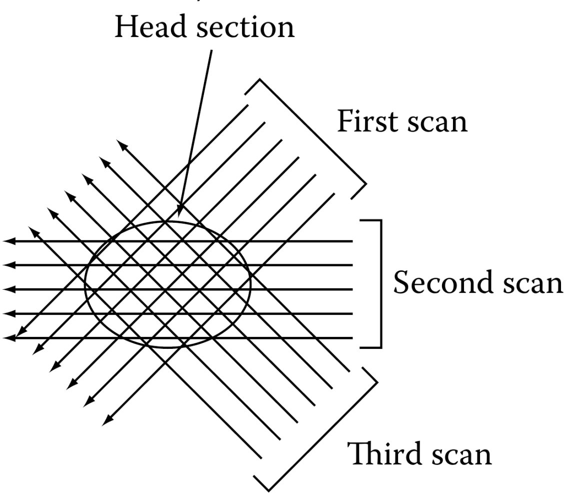

1. Sequence of parallel sections *(tomos)*
2. Sequence of projections from multiple directions

CT principles

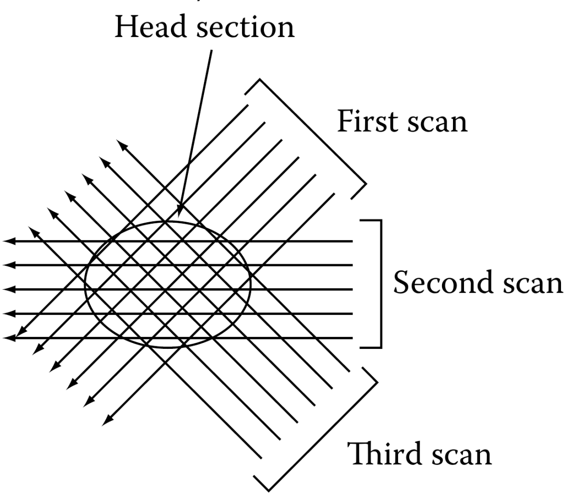

1. Sequence of parallel sections *(tomos)*
2. Sequence of projections from multiple directions
3. Reconstruction of the object

CT example scans

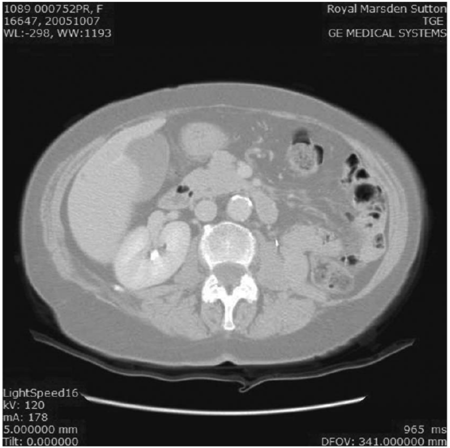

Head and kidneys

CT example scans

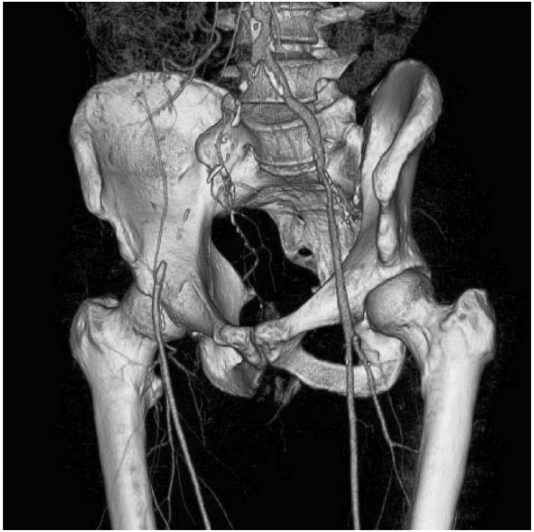

CT angiography, pelvis

Clinical applications

- Lungs

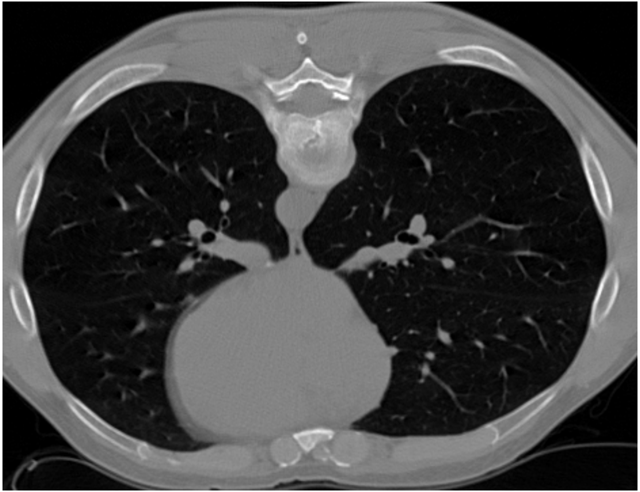

Clinical applications

- Lungs

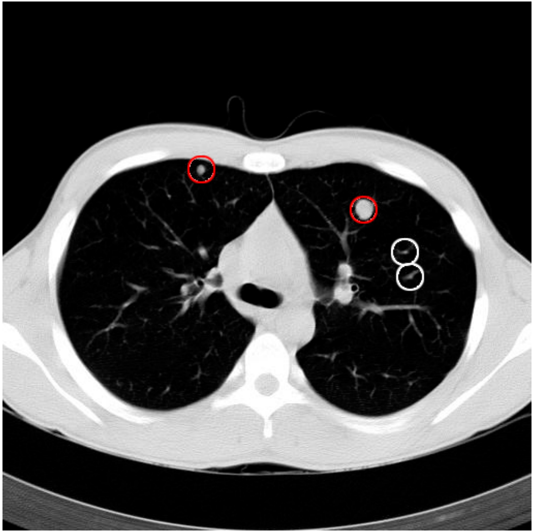

Clinical applications

- Lungs
- Head

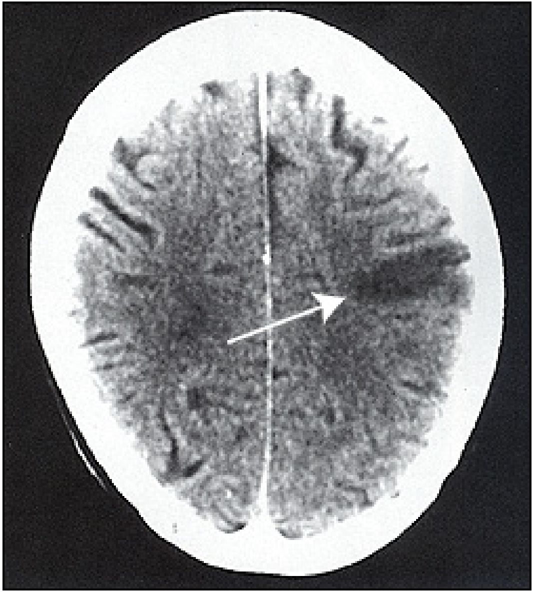

Clinical applications

- Lungs
- Head

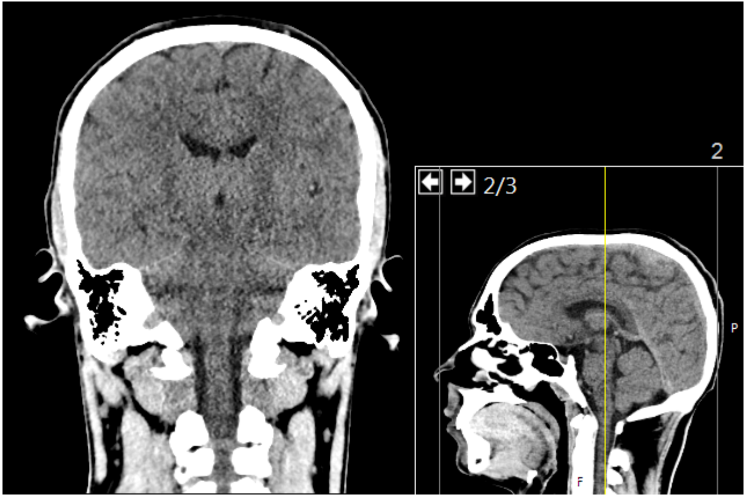

Clinical applications

- Lungs
- Head

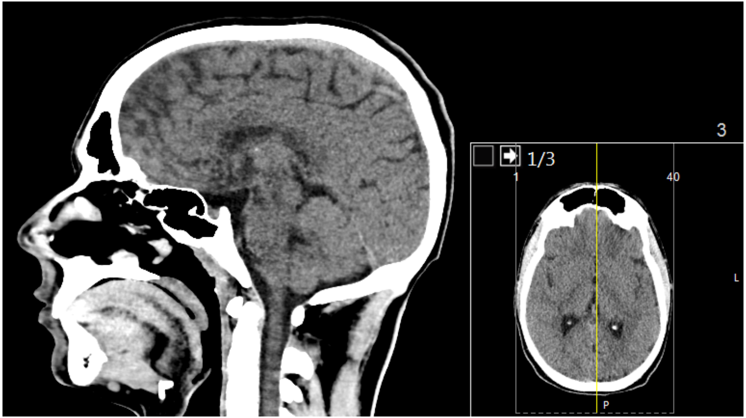

Clinical applications

- Lungs
- Head
- Abdomen

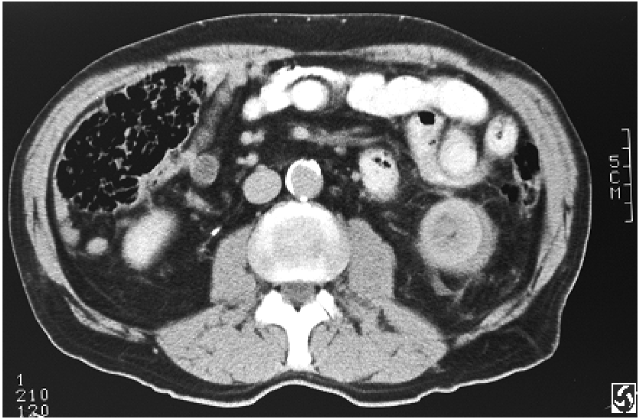

Tomography modalities

- X-rays — CT
- gamma rays — PET, positron emission tomography
- gamma rays — SPECT, single-photon emission computerized tomography
- light — optical tomography
- RF waves — MRI, magnetic resonance imaging
- DC — electric impedance tomography
- ultrasound — ultrasound tomography

First scanner

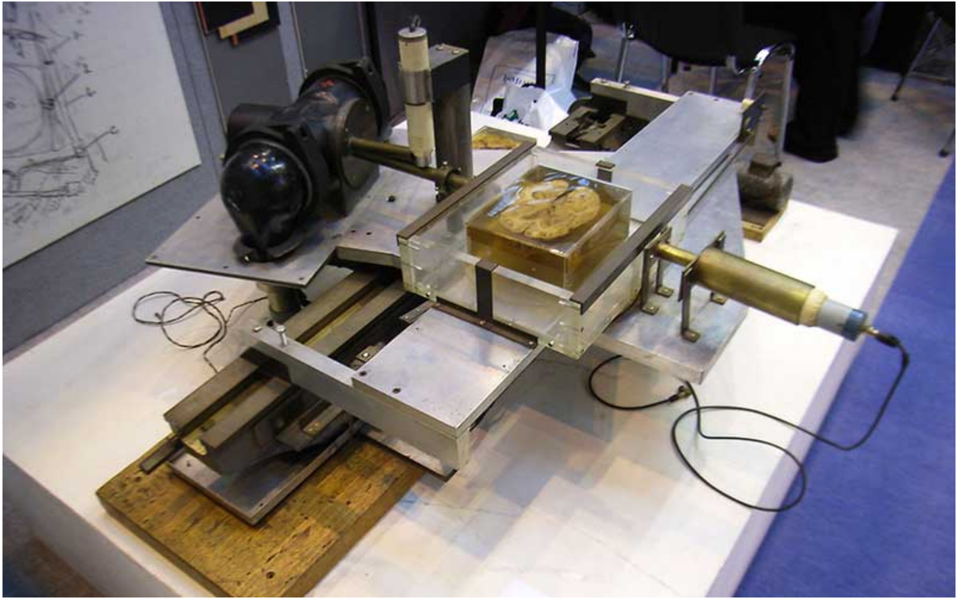

Scanner geometry — generation 1

1971

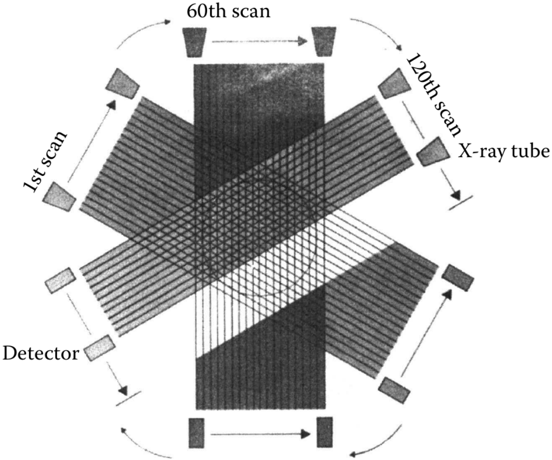

- Single source and single detector
- Finely collimated narrow beam
- Alternating translation and rotation
- Very slow (4 min / section), low resolution
- Low cost, good scatter rejection, easy calibration

Scanner geometry — generation 2

1974

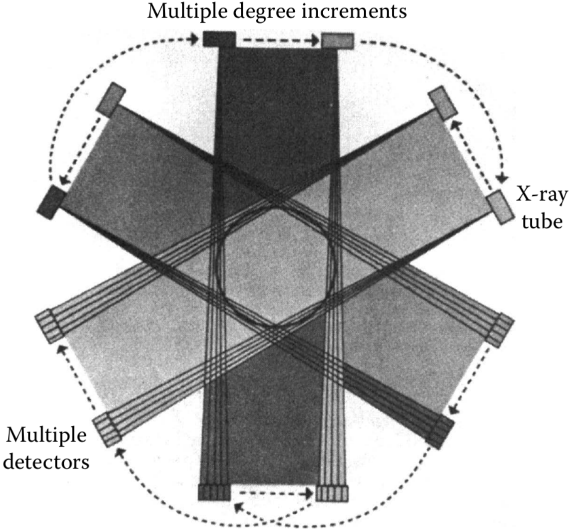

- Narrow fan beam ($\sim 10^\circ$), multiple detectors (N)
- N projections acquired in parallel
- Increased rotation increment
- Increased speed (20 s / section)

Scanner geometry — generation 3

1975

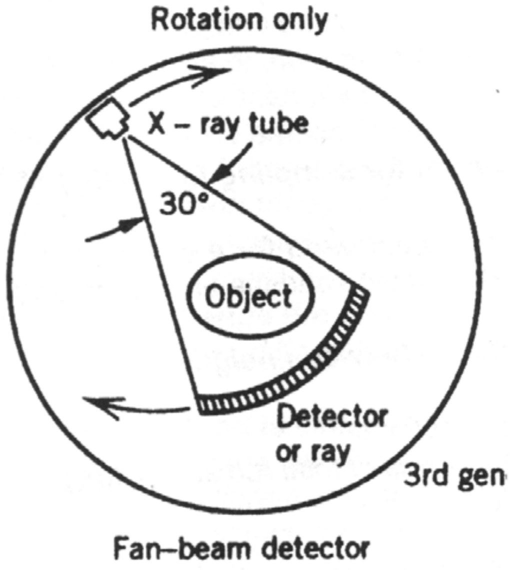

- Wide fan beam ($30^\circ \sim 60^\circ$) covering complete field of view
- 100s of detectors
- Only rotation, no translation
- Pulsed or continuous acquisition
- Fast (5 s / section)
- Cone beam geometry
- Most frequently used

Scanner geometry — generation 4

1977

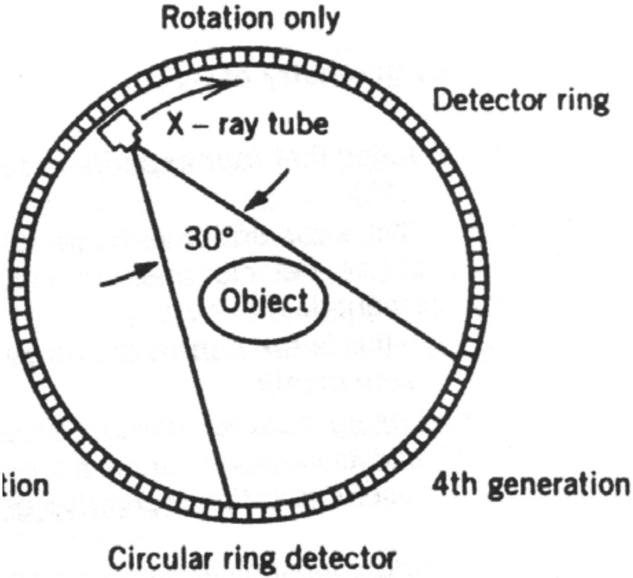

- Rotating source, stationary detector rings
- More expensive
- Avoids rotating contacts
- Fast

Electron beam CT
(EBCT, 1983)

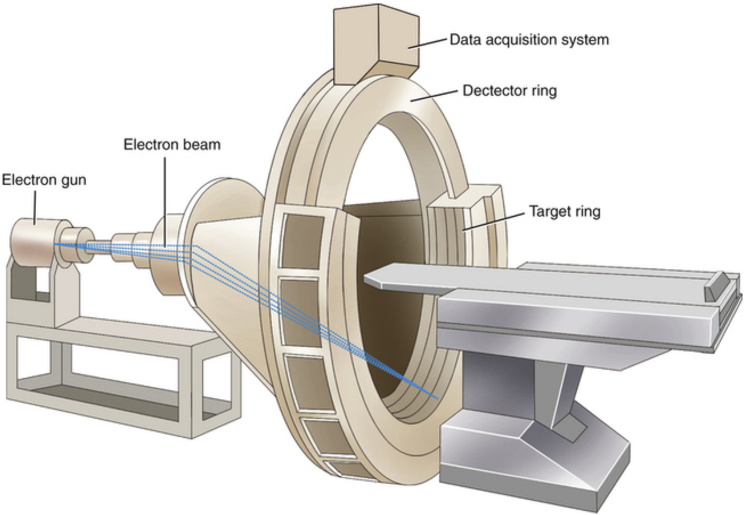

- No moving parts
- Directional X-ray source
- Extremely fast (beating heart)
- Lower signal to noise ratio and spatial resolution

CT X-ray sources

Similar but bigger than radiography X-ray sources

Typical properties of an X-ray tube used for CT compared to those of a conventional radiographic tube.

	Conventional X-Ray Tube	CT X-Ray Tube
Typical exposure parameters	70 kV, 40 mAs	120 kV, 10,000 mAs
Energy requirements	2,800 J	1,200,000 J
Anode diameter	100 mm	160 mm
Anode heat storage capacity	450,000 J	3,200,000 J
Maximum anode heat dissipation	120,000 J/min	540,000 J/min
Maximum continuous power rating	450 W	4000 W
Cooling method	Fan	Circulating oil

- Challenges: Power leads, cooling, vibration, ...

CT X-ray sources

Similar but bigger than radiography X-ray sources

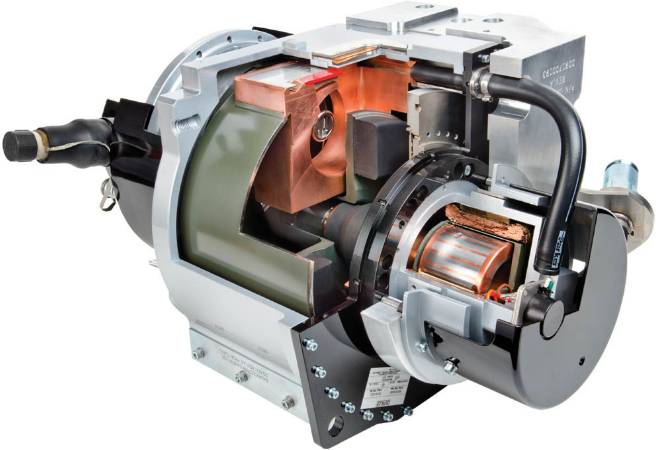

- Challenges: Power leads, cooling, vibration, ...

CT X-ray sources (future?)

Liquid anode tube: overcoming power density limitations of solid target X-ray tubes

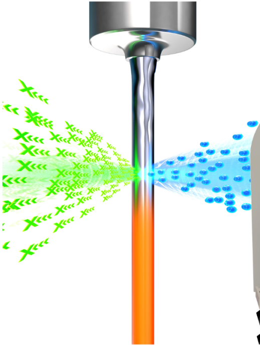

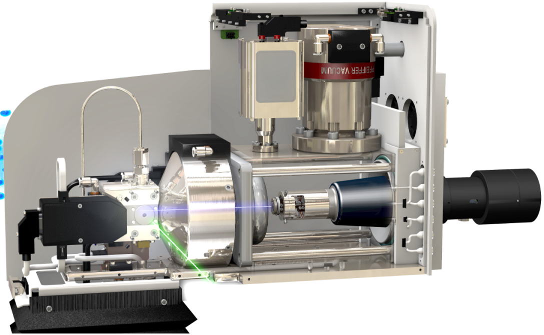

- Tin, gallium, indium, ...
- Heat dissipation problem nearly obsolete
- Small focal sizes viable (10-15µm) at high power ($\sim$ 500 W)
  $\Rightarrow$ Allows for high magnification / system resolution

Filtering and collimation (1)

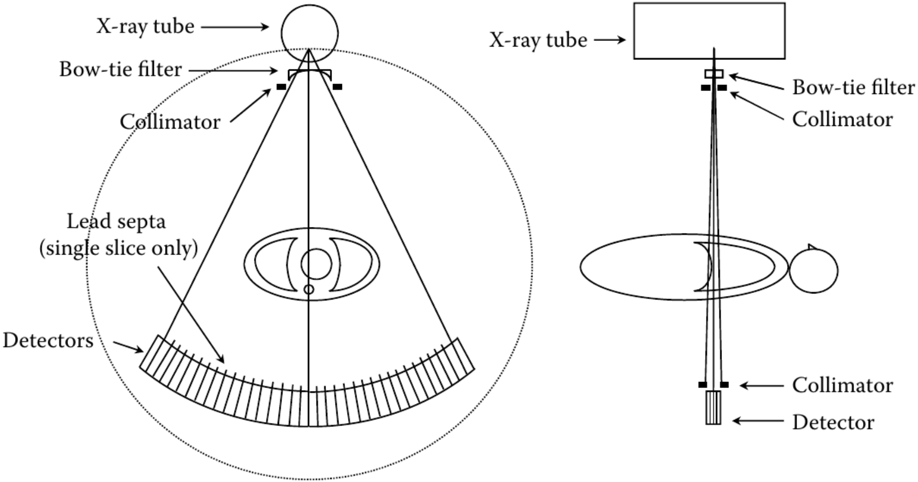

Filtering and collimation (2)

- Beam shaping (attenuate lateral part of the beam)

- Pre-patient and detector collimation — beam(slice) width

CT detector types

- Xenon ionization chamber detectors
  - Faster but less sensitive
- Scintillation detectors
  - More sensitive but slower (afterglow, scintillator dependent)

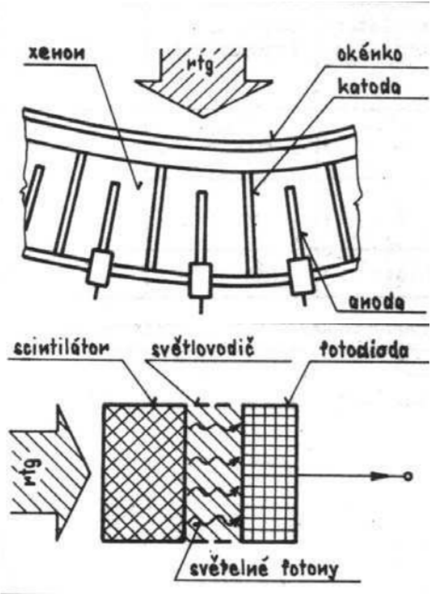

CT detector types

Properties of detectors in common use in CT scanning.

	Xenon Detectors	**Crystal Scintillator**	**Ceramic Scintillator**
Detector	High pressure (8–25 atm) Xe ionisation chamber	$CaWO_4$ + silicon photodiode	Gd_2O_2S + silicon photodiode
Detector array	Single chamber, divided into elements by septa	Discrete detectors	Discrete detectors
Signal	Proportional to ionisation intensity	Proportional to light intensity	Proportional to light intensity
Detector efficiency	40%–70%	95%–100%	90%–100%
Geometric efficiency (in fan direction)	>90%	>80%	>80%
Afterglow limitations	No	Yes	No
Detector matching	No	Yes	Yes

Scintillation detector construction

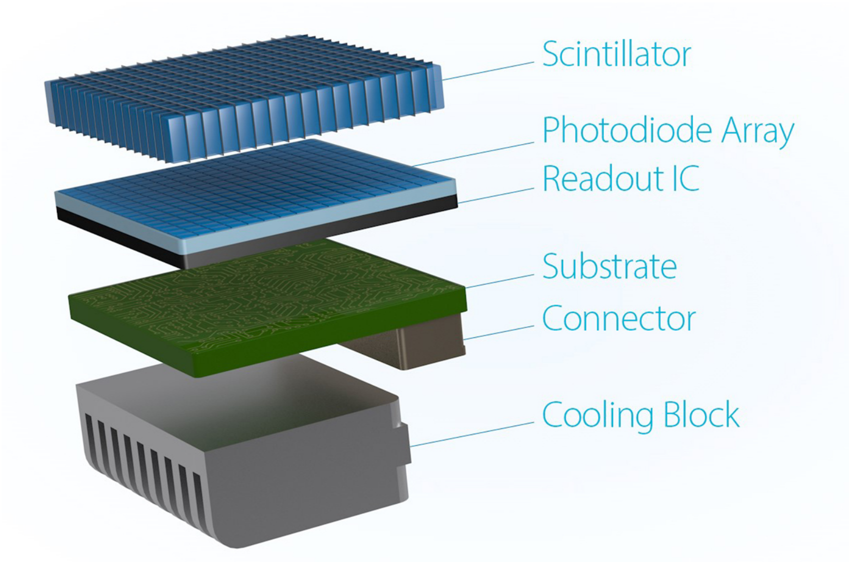

Scintillation detector construction

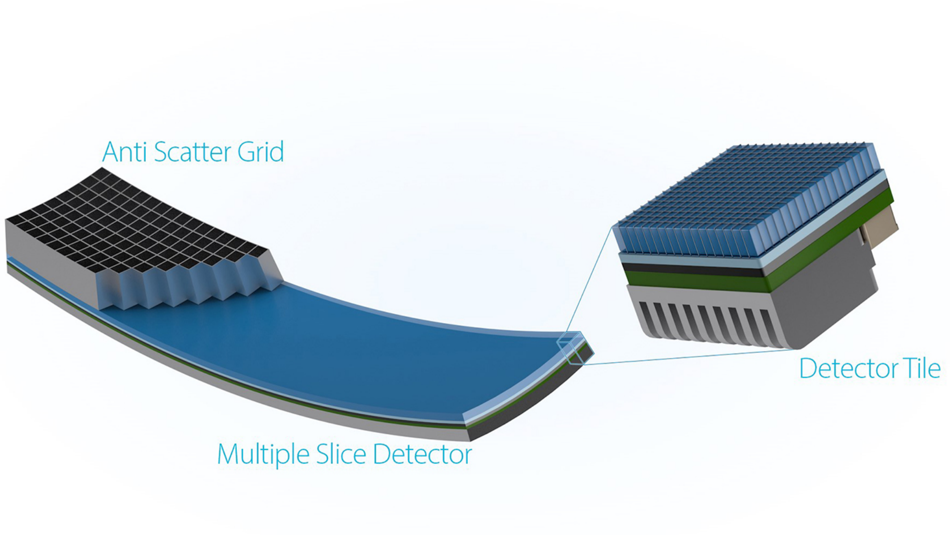

Multiple (e.g. 32, 64) slices $\longrightarrow$ acceleration

Scintillation detector construction

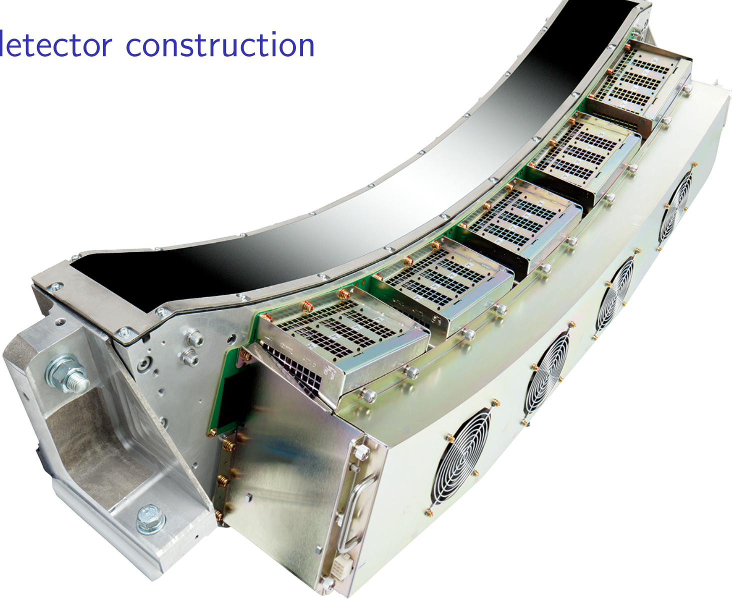

Multiple (e.g. 32, 64) slices $\longrightarrow$ acceleration

X-ray detectors: Photon counting detectors

e.g. Timepix/Medipix

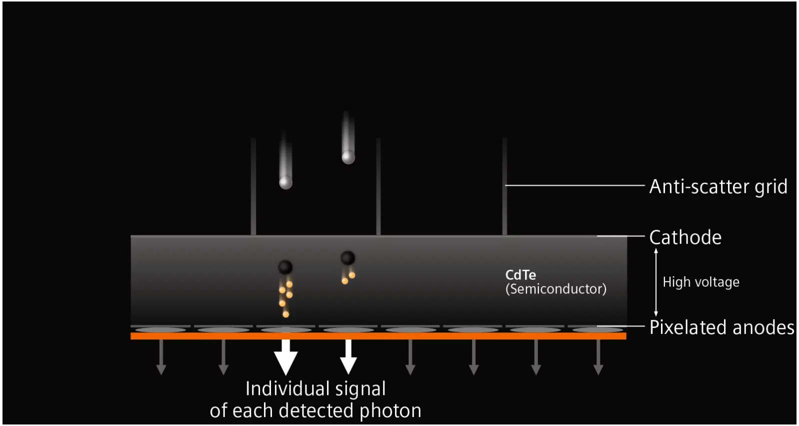

- Unlimited dynamic range and exposure time
- Detected count obeys Poisson distribution

Electric processing — corrections

- Offset correction (zero signal at rest)
- Normalization correction (x-ray source intensity fluctuation)
- Sensitivity correction (inhomogeneous detectors and amplifiers)
- Geometric correction
- Beam hardening correction
- Cosine correction (for fan beam geometry)

Attenuation along a line

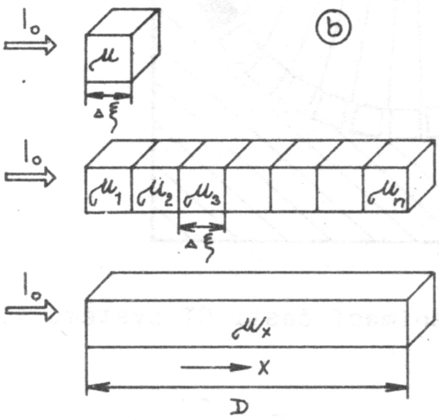

Homogeneous material (Beer-Lambert's law)

$$I = I_0 \mathrm{e}^{-\mu \Delta\xi}$$

Piecewise homogeneous material

$$I = I_0 \prod_{i=1}^{n} \mathrm{e}^{-\mu\Delta\xi} = I_0 \mathrm{e}^{-\Delta\xi \sum_{i=1}^{n} \mu_i}$$

Continuously varying $\mu(x)$, $x = i\Delta\xi$

$$\begin{aligned} I &= I_0 \mathrm{e}^{-\lim_{\Delta\xi \to 0} \Delta\xi \sum_{i=1}^{n} \mu_i} \\ &= I_0 \mathrm{e}^{-\int_0^D \mu(x)\mathrm{d}x} \end{aligned}$$

Line integral for line L

$$I = I_0 \mathrm{e}^{-\int_L \mu(\mathbf{x})\mathrm{d}\mathbf{x}}$$

Hounsfield units

HU, CT number

$$CT = 1000 \frac{\mu - \mu_{\text{water}}}{\mu_{\text{water}}}$$

- Values between -1000 (air) and approximately 1000 (bones)
- Densities in HU are *reproducible* between devices
- To differentiate soft tissue types, tumor types etc.
- Accurate calibration is needed

Hounsfield units

HU, CT number

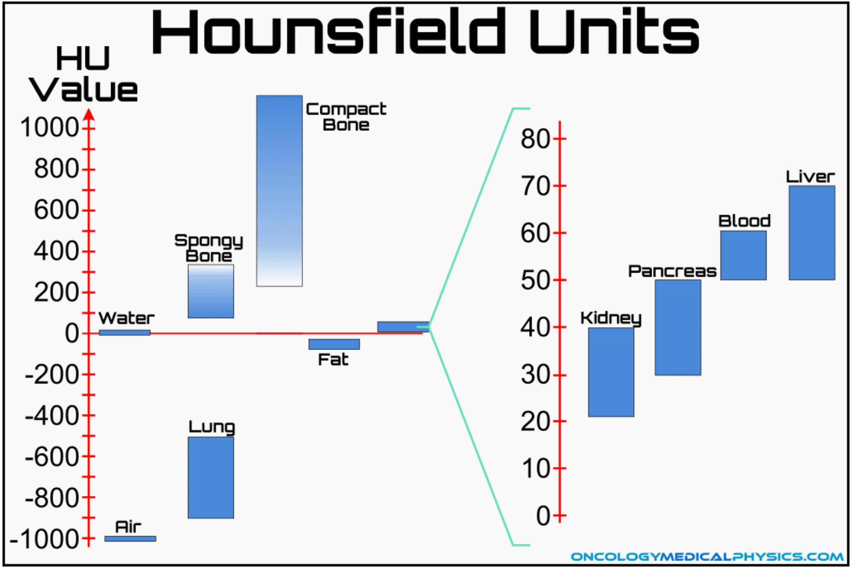

Attenuation descreases with E

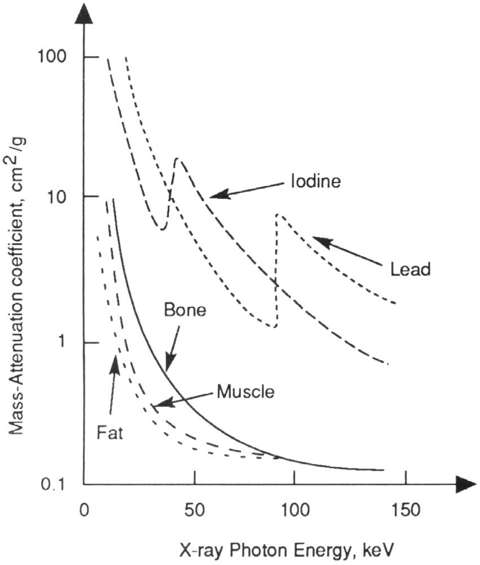

Attenuation, interaction types

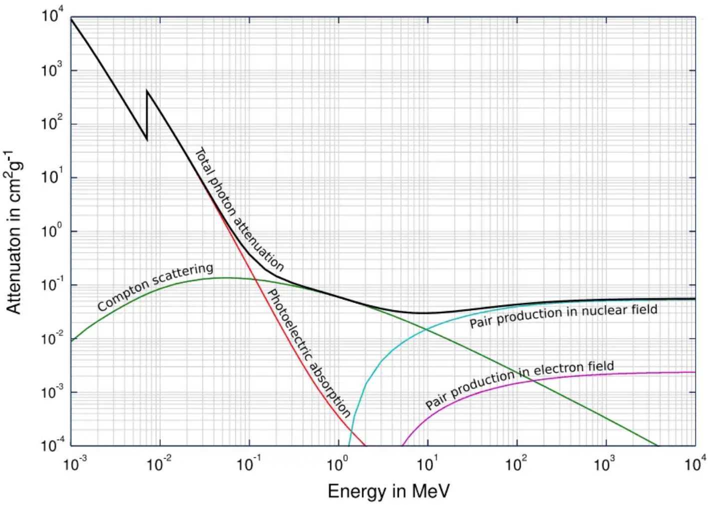

Attenuation, materials

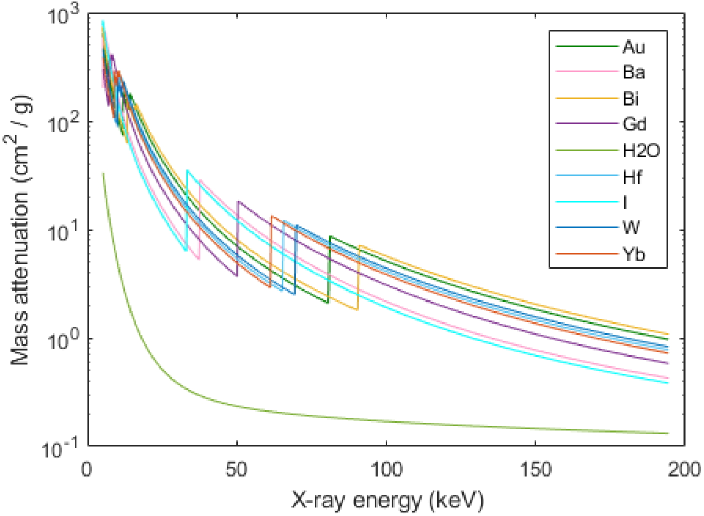

- "absorption edges" correspond binding energies of electrons from atom's shells.

Beam hardening

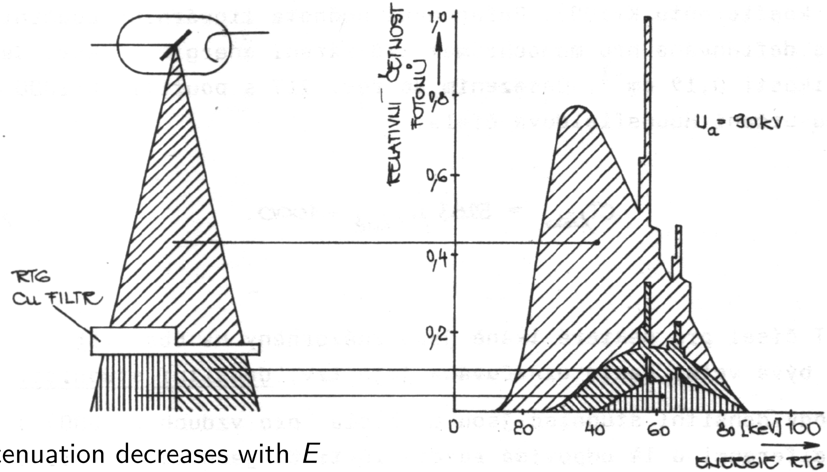

- Attenuation decreases with E
- $\longrightarrow$ low E rays are attenuated more
- $\longrightarrow$ mean E increases

Beam hardening

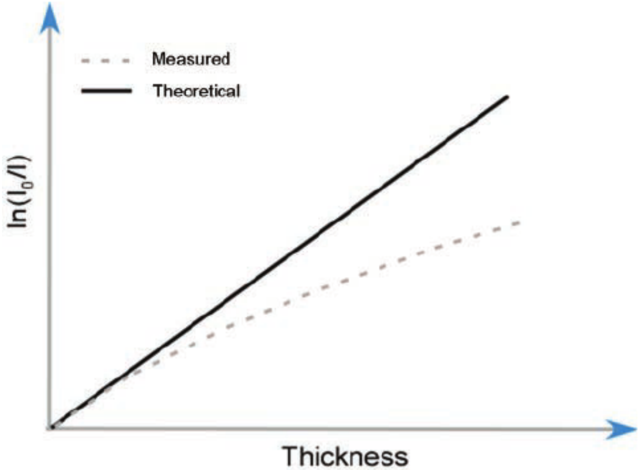

- Measured attenuation $p = \log(I_0/I) <$ theoretically linear $\mu\Delta\xi$.
- Beam hardening correction

Linear forward problem

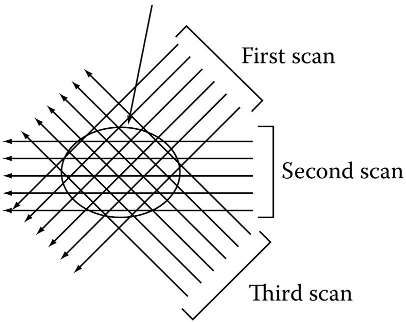

For N straight lines L_j, measure the attenuation

$$p_j = \log \frac{I_0^j}{I^j} = \int_{L_j} \mu(\mathbf{x})\mathrm{d}\mathbf{x}$$

Assumptions

- Infinitely thin rays
- Straight lines — no scattering, reflection or refraction
- Monochromatic radiation — no beam hardening

(Assumptions can be relaxed but more complicated dependency.)

Linear forward problem

For N straight lines L_j, measure the attenuation

$$p_j = \log \frac{I_0^j}{I^j} = \int_{L_j} \mu(\mathbf{x}) \mathrm{d}\mathbf{x}$$

Assumptions

- Infinitely thin rays
- Straight lines — no scattering, reflection or refraction
- Monochromatic radiation — no beam hardening

(Assumptions can be relaxed but more complicated dependency.)

Discretization

$$\mu(\mathbf{x}) = \sum_{i=1}^{M} c_i \psi_i(\mathbf{x}) \quad \text{with pixels } \psi_i$$

$\longrightarrow$ linear system of equations $\mathbf{L}\mathbf{c} = \mathbf{p}$

Integration lines in polar coordinates

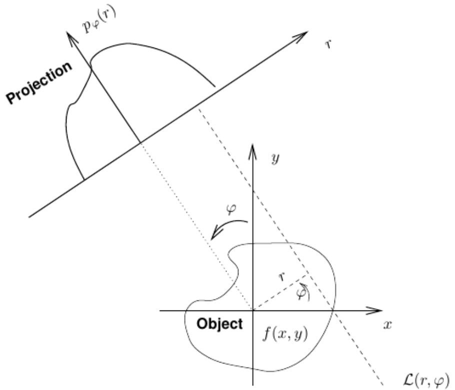

Describe integration lines by angle φ and offset r:

$$\begin{aligned} L(\varphi, r) &= \{(x, y) \in \mathbb{R}^2;\ x \cos\varphi + y \sin\varphi = r\} \\ &= \{(r\cos\varphi - t\sin\varphi, r\sin\varphi + t\cos\varphi);\ t \in \mathbb{R}\} \end{aligned}$$

Integration lines in polar coordinates

Describe integration lines by angle φ and offset r:

$$\begin{aligned} L(\varphi, r) &= \{(x, y) \in \mathbb{R}^2;\ x\cos\varphi + y\sin\varphi = r\} \\ &= \{(r\cos\varphi - t\sin\varphi, r\sin\varphi + t\cos\varphi);\ t \in \mathbb{R}\} \end{aligned}$$

Implicit line equation, $\mathbf{x} = (x, y)$

$$\begin{bmatrix}\cos\varphi, & \sin\varphi\end{bmatrix}\mathbf{x} = 0$$

Parametric line equation

$$\underbrace{\begin{bmatrix}\cos\varphi & -\sin\varphi \\ \sin\varphi & \cos\varphi\end{bmatrix}}_{\text{rotation matrix } R(\varphi)} \begin{bmatrix} r \\ t \end{bmatrix} = \mathbf{x}$$

Rotating system of coordinates

$$\begin{bmatrix} \xi \\ \eta \end{bmatrix} = R(\varphi) \begin{bmatrix} \xi' \\ \eta' \end{bmatrix}$$

$$\begin{bmatrix} \xi' \\ \eta' \end{bmatrix} = R^T(\varphi) \begin{bmatrix} \xi \\ \eta \end{bmatrix}$$

$$R^T(\varphi) = R(-\varphi)$$

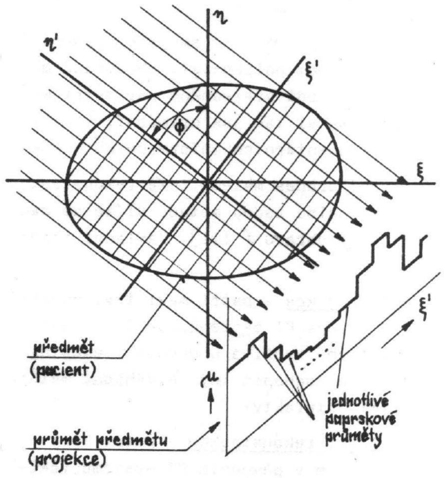

Projection

$$P_\varphi(\xi') = \int_{L(\varphi,\xi')} \mu(\mathbf{x})\mathrm{d}\mathbf{x} = \int o(\xi', \eta')\mathrm{d}\eta'$$

Measurements

$$P_\varphi(\xi') = \log \frac{I_0}{I(\varphi, \xi')}$$

Change of variables

$$\xi' = r, \quad \eta' = t, \quad x = \xi, \quad y = \eta$$

Radon transform

Projection in polar coordinates:

$$P_\varphi(\xi') = \mathscr{R}\left[o(\xi,\eta)\right]$$
$$P_\varphi(\xi') = \int_L o(\xi,\eta)\mathrm{d}l$$

along the line L defined by φ a ξ':

$$\xi' = \xi\cos\varphi + \eta\sin\varphi$$

Equivalently

$$P_\varphi(\xi') = \int o(\xi'\cos\varphi - \eta'\sin\varphi, \xi'\sin\varphi + \eta'\cos\varphi)\mathrm{d}\eta'$$

Radon transform properties

- Function f — unknown density, Radon transform — projection data.
- inverse of the Radon transform — reconstruction

Properties

- **Linearity:**

$$\mathscr{R}[\alpha f + \beta g] = \alpha \mathscr{R}[f] + \beta \mathscr{R}[f]$$

- **Periodicity:**

$$P_{\varphi}(\xi') = P_{\varphi \pm 2\pi}(\xi') = P_{\varphi \pm \pi}(-\xi')$$

... and many others

Radon transform of a point

$$o(\xi, \eta) = \delta(\xi - \xi_0, \eta - \eta_0)$$
$$P_\varphi(\xi') = \mathscr{R}\big[o(\xi, \eta)\big] = \delta\big(\xi_0 \cos\varphi + \eta_0 \sin\varphi - \xi'\big)$$

...is a sinusoid with amplitude $\sqrt{\xi_0^2 + \eta_0^2}$ and phase $\angle(\xi_0, \eta_0)$.

$$\xi' = \xi_0 \cos\varphi + \eta_0 \sin\varphi$$

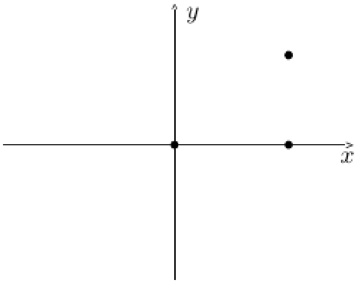

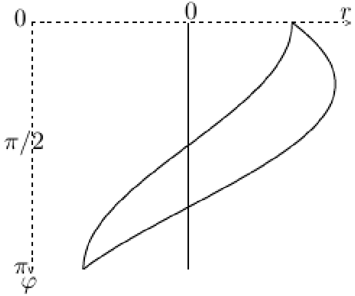

Radon transform
(sinogram)

of a disc

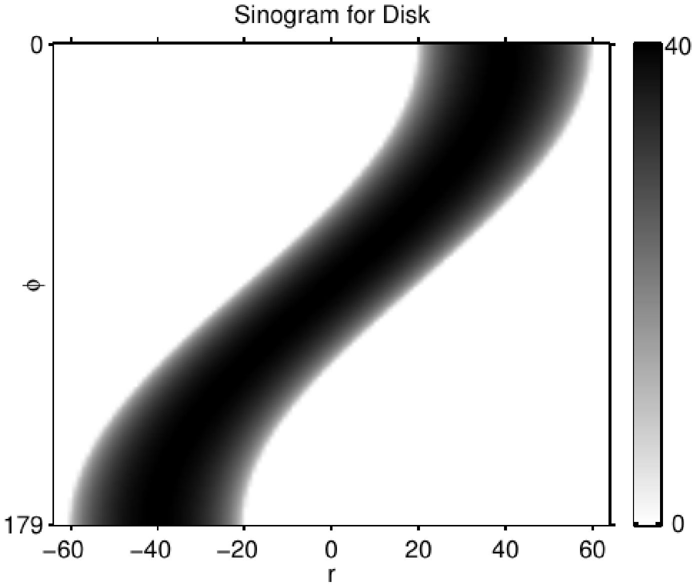

Radon transform

(sinogram)

of a square
(inverted)

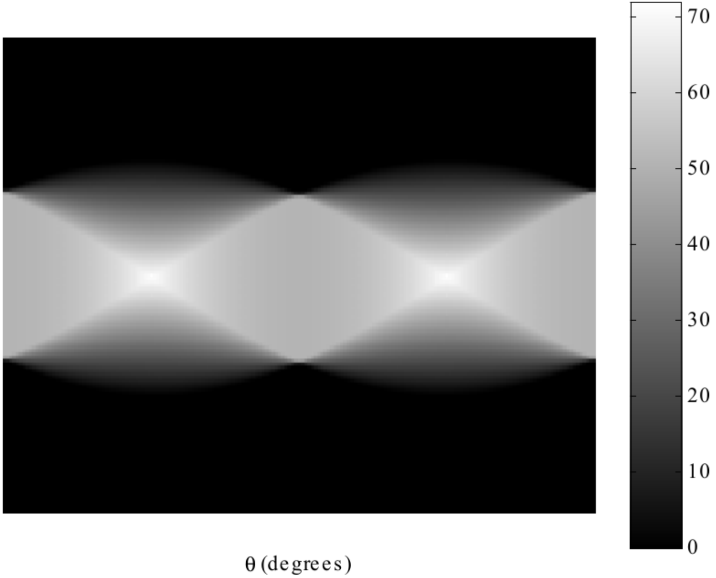

Radon transform
(sinogram)

of an object with inserts (inverted)